Activation of LXRs alleviates neuropathic pain-induced cognitive dysfunction by modulation 2 of microglia polarization and synaptic plasticity via PI3K/AKT pathway.

Title page

Activation of LXRs alleviates neuropathic pain-induced cognitive dysfunction by modulation of microglia polarization and synaptic plasticity via PI3K/AKT pathway

Siyi Han[1], Xiaoman Yuan[1], Fengtian Zhao[1], Anne Manyande[2], Feng Gao[1], Jie Wang[3], Wen Zhang[1,*], Xuebi Tian[1,*]

[1] Department of Anesthesiology, Hubei Key Laboratory of Geriatric Anesthesia and Perioperative Brain Health, and Wuhan Clinical Research Center for Geriatric Anesthesia, Tongji Hospital, Tongji Medical College, Huazhong University of Science and Technology, Wuhan, Hubei, China

[2] School of Human and Social Sciences, University of West London, London, UK

[3.] Wuhan Institute of Physics and Mathematics, Chinese Academy of Sciences, Wuhan, Hubei, China

***Corresponding author**

1. Wen Zhang

Email: wenzhang@tjh.tjmu.edu.cn

Address: Tongji Hospital, Tongji Medical College, Huazhong University of Science & Technology, No.1095 Jiefang Avenue, Wuhan, Hubei Province, China

2. Xuebi Tian

Email: tianxb@hust.edu.cn;

Tel: +86-27-83663282; Fax: +86-27-83663173

Address: Tongji Hospital, Tongji Medical College, Huazhong University of Science & Technology, No.1095 Jiefang Avenue, Wuhan, Hubei Province, China

Funding:

This work was supported by the National Natural Science Foundation of China (No. 81974170)

and the Natural Science Foundation of Hubei Province (2021CFB341)

Data availability:

All data relevant to the study are included in the article or uploaded as supplementary information.

Data is available upon request.

Declarations:

Conflict of interest: The authors declare no conflicts of interest.

Activation of LXRs alleviates neuropathic pain-induced cognitive dysfunction by modulation of microglia polarization and synaptic plasticity via PI3K/AKT pathway

Abstract

Objective:

Cognitive dysfunction is a common comorbidity in patients with chronic pain. Activation of Liver X receptors (LXRs) plays a potential role in improving cognitive disorders in central nervous diseases. In this study, we investigated the role of LXRs in cognitive deficits induced by neuropathic pain.

Methods:

We established the spared nerve injury (SNI) model to investigate pain-induced memory dysfunction. Pharmacological activation of LXRs with T0901317 or inhibition with GSK2033 was applied. PI3K inhibitor LY294002 was administered to explore the underlying mechanism of LXRs. Changes in neuroinflammation, microglia polarization, and synaptic plasticity were assessed using biochemical technologies.

Results:

We found that SNI-induced cognitive impairment was associated with reduced LXRβ expression, increased M1-phenotype microglia, decreased synaptic proteins, and inhibition of PI3K/AKT signaling pathway in the hippocampus. Activation of LXRs using T0901317 effectively alleviated SNI-induced cognitive impairment. Additionally, T0901317 promoted the polarization of microglia from M1 to M2, reduced pro-inflammatory cytokines, and upregulated synaptic proteins in the hippocampus. However, administration of GSK2033 or LY294002 abolished these protective effects of T0901317 in SNI mice.

Conclusions:

LXRs activation alleviates neuropathic pain-induced cognitive impairment by modulating microglia polarization, neuroinflammation, and synaptic plasticity, at least partly via acitvation of PI3K/AKT signaling in the hippocampus. LXRs may be promising targets for addressing pain-related cognitive deficits.

Keywords:

Liver X receptors; Neuropathic pain; Microglia polarization; Cognitive dysfunction; Neuroinflammation; Synaptic plasticity

1. Introduction

Pain has become an increasingly significant public health concern, as pain-related diseases have become a leading cause of disability and disease globally [1]. Clinical studies have revealed that chronic pain often combines with cognitive disorders including impairments in learning and memory, attention, and executive function [2, 3]. However, the mechanism underlying pain-induced cognitive dysfunction remains poorly understood, and effective treatments for addressing this condition are still lacking.

It has been noticed that chronic pain induces neuroinflammation in the supraspinal regions, particularly in the hippocampus and medial prefrontal cortex, which are critical in learning and memory processes [4, 5]. Elevated levels of pro-inflammatory factors in the hippocampus, such as tumor necrosis factor-alpha (TNF-α) and interleukin (IL)-1β, contribute to the development of cognitive disorders in animal models of neuropathic pain [6, 7]. In the central nervous system (CNS), microglia serve as key modulators of neuroinflammation and can shift between pro-inflammatory (M1) and anti-inflammatory (M2) phenotypes depending on their activation status in pathological conditions [8, 9]. Preclinic studies have demonstrated that pharmacological elimination of microglia prevents memory deficits induced by chronic pain [6, 10]. However, it would be better to modulate the transformation of microglia from M1 to M2 to promote their neuroprotective effects [11].

Prolonged neuroinflammation in the hippocampus is often accompanied by disorders of synaptic plasticity [12, 13]. Chronic pain significantly influences synaptic plasticity in the hippocampus, leading to altered long-term potentiation (LTP), reduced spine density, and impaired neurogenesis [14–16]. It is well-established that dysfunction in hippocampal synaptic plasticity

leads to memory impairment in nerve-injured mice [17, 18]. Therefore, a comprehensive approach that targets various aspects, such as neuroinflammation and synaptic plasticity, is necessary for the treatment of pain-related cognitive deficits.

Liver X receptors (LXRs), including LXRα and LXRβ, are transcription factors within the nuclear receptor superfamily [19]. LXRα is the main subtype in the liver and adipose tissue, while LXRβ is widely expressed and especially abundant in the brain [20]. Recent studies have highlighted the beneficial effects of LXRs on multiple neurologic diseases, given their central roles in lipid metabolism and inflammatory signaling [21, 22]. LXRs agonist T0901317 has been shown to enhance cholesterol efflux and transportation, resulting in reduced β-amyloid levels [23], as well as attenuated neuronal apoptosis [24] and neuroinflammation [25]. Moreover, research demonstrated that LXRβ deletion leads to cognitive impairment in mice, while activation of LXRs with GW3965 ameliorates sleep deprivation-induced cognitive impairment by inhibiting microglia activation and inflammatory factors in the hippocampus [26]. Importantly, LXRs activation plays a anti-depressive role by suppressing microglial M1-polarization and promoting synaptic plasticity in the hippocampus [27]. However, the potential neuroprotective role of LXRs after neuropathic pain remains to be elucidated.

Studies have also indicated that LXRs agonists promote hippocampal neurogenesis [28] and synaptic plasticity [29] by activating phosphatidylinositol 3-kinase (PI3K) /protein kinase B (AKT) signaling pathway. Moreover, as a lipid kinase, PI3K also plays important roles in mediating extracellular signals to regulate cell growth and differentiation, as well as microglial phenotype [30]. In both in vitro and in vivo experiments, activation of PI3K/AKT signaling pathway has been demonstrated to inhibit microglial M1 polarization and suppress microglia-mediated

104 neuroinflammation [31, 32]. Therefore, we hypothesized that PI3K/AKT pathway may underlie
105 the mechanism responsible for the neuroprotective and anti-inflammatory effects of LXRs
106 activation.

107 In this study, we characterized changes in LXRs expressions in the hippocampus of mice with
108 neuropathic pain and investigated their effects on cognitive performance. We found that activation
109 of LXRs alleviates cognitive dysfunction in SNI mice by modulating microglial polarization and
110 enhancing synaptic plasticity in the hippocampus through the activation of PI3K/AKT signaling
111 pathway.

112 **2. Materials and Methods**

113 **2.1 Animals**

114 Male C57 BL/6J (8 weeks, 20-25g) were purchased from Tongji Hospital, Tongji Medical
115 College, Huazhong University of Science and Technology. All mice were housed 5 per cage in a
116 temperature-controlled room and provided *ad libitum* access to water and food. The mice were
117 maintained under a 12-hour light/dark cycle. All experimental procedures were approved by the
118 Animal Care and Use Committee of Tongji Hospital.

119 **2.2 Animal model of neuropathic pain**

120 Under pentobarbital sodium anesthesia (50 mg/kg, intraperitoneally (*i.p.*)), mice underwent
121 spared nerve injury (SNI) surgery. In brief, the left thigh skin and muscle were incised to expose
122 the sciatic nerve, which includes the sural, common peroneal, and tibial nerves. The common
123 peroneal and tibial nerves were ligated with 6.0 sutures, and then cut off, with about a 2 mm
124 section of the distal nerve stump being removed. The skin was finally closed and disinfected with
125 iodophor. Throughout the surgery, the sural nerve was carefully protected to avoid stretching or

impairment. In the Sham group, all nerves were left intact.

2.3 Experimental designs and drugs treatment

This study comprises four experiments, with mice randomly assigned to different groups.

Experiment 1

To evaluate changes in LXRs expression, microglia polarization, synaptic plasticity and cognitive function after SNI, mice were allocated to the following 2 groups (Fig. 1A): (1) Sham group; (2) SNI group (n = 9/group).

Experiment 2

To determine the effects of LXRs activation with T0901317, mice were allocated to the following 4 groups (Fig. 5A): (1) Sham + Vehicle group; (2) Sham + T0901317 group; (3) SNI + Vehicle group; (4) SNI + T0901317 group (n = 9/group). We dissolved T0901317 (MedChemExpress, USA) in 5% DMSO with normal saline at a concentration of 5 mg/ml. T0901317 (30 mg/kg) or 5% DMSO with normal saline as a vehicle was administered *i.p.* once a day for 14 days [33].

Experiment 3

To further confirm the neuroprotective effects of T0901317, we applied LXRs antagonist GSK2033 in SNI mice. After the implantation of a cannula in the lateral ventricles, mice were allocated to the following 4 groups (Fig. 7A): (1) SNI + Vehicle group; (2) SNI + T0901317 group; (3) SNI + GSK2033 group; (4) SNI + GSK2033 + T0901317 group (n = 9/group). GSK2033 (MedChemExpress, USA) was dissolved in 0.1% DMSO with normal saline at a concentration of 3 mg/ml. GSK2033 (0.3 mg/kg) or an equal volume of vehicle (0.1% DMSO) was intracerebroventricularly (*i.c.v.*) administered 30 min before surgery and days 7 and 14 after

surgery [27]. T0901317 (30 mg/kg) or vehicle (5% DMSO) was administered i.p. once daily for 14 days.

Experiment 4

To explore the downstream mechanism of LXRs, we administered the PI3K inhibitor LY294002 (Fig. 9A). After the implantation of a cannula in the lateral ventricles, mice were divided into 4 groups: (1) SNI + Vehicle group; (2) SNI + T0901317 group; (3) SNI + LY294002 group; (4) SNI + LY294002 + T0901317 group. LY294002 (MedChemExpress, USA) was dissolved in 0.1% DMSO with normal saline at a concentration of 10 mM (2 μL) [34] and injected into the lateral ventricle of mice 30 min before the application of T0901317 for 14 days. Additional details of drug administration in the experiment 3 and 4 are shown in Supplementary Table 1.

2.4 Behavioral tests

All behavioral procedures were conducted in a room at constant temperature (22 ± 1 ℃) between 8:00 AM and 17:00 PM and the brightness was maintained at 50 lux.

Pain behavioral test

Von Frey filaments were applied to measure the ipsilateral hind paw mechanical withdrawal threshold (MPWT). Mice were placed on the soft wire mesh floor in individual plastic boxes to habituate for 30 min. Von Frey filaments were used in ascending order of forces from 0.008 g to 1 g to stimulate the lateral plantar surface of the left hind paw. Positive reactions were manifested as rapid paw withdrawal, shaking, or licking upon the application or prompt removal of the filaments. The MPWT was defined as the lowest amount of force that elicited a positive reaction at least 3 times out of 5 repetitive stimuli.

Open field test (OFT)

The OFT was conducted 15 days after surgery to evaluate the locomotor activity of SNI mice. Mice were placed in an open field apparatus (40 × 40 × 50 cm^2) and allowed to explore freely for 5 min. The locomotion of mice was measured by the ANY-maze software (Stoelting, USA). The surface of the apparatus was cleaned with 75% alcohol to remove olfactory cues after each test.

Novel object recognition test (NORT)

To assess learning and memory function, the NORT was performed 1 h after the OFT. As described previously [35], in the training stage, mice were allowed to explore two identical rectangular objects A and B placed in the apparatus for 5 min. The testing phase was carried out 24 h after the training phase. The familiar object B was replaced by a novel cylinder (object C), and mice were allowed to explore for 5 min again. Cognitive function was evaluated by calculating the discrimination ratio (DR), defined as C/ (A + C). C is the time spent exploring the novel object. A is the time spent exploring the familiar object, and A + C is the total time spent exploring the two objects in the testing phase. The samples for biochemical analysis were collected immediately after the behavioral tests.

2.5 Cannulation and intracerebroventricular interventions

After being anesthetized as mentioned above, mice were placed on a stereotaxic frame (RWD Life Science Co., Ltd, China). A brain infusion cannula was implanted in the left lateral ventricle (AP: -s0.34 mm, ML: -1 mm, DV: -2.5 mm) according to the mouse brain atlas of Franklin and Paxinos. The cannulas were fixed to the skull using glue and dental cement. The SNI surgery was conducted after a week of recovery, and LXRs antagonist GSK2033 or PI3K inhibitor LY294002 was administered via a pump at the rate of 500 nl/min. The position of the placed cannula was confirmed by immunofluorescence staining (Supplementary Fig. 1).

2.6 Western blot

The bilateral hippocampus protein samples were prepared as previously described [36]. Equal quantities of total protein were separated using SDS-PAGE gels and then transferred to polyvinylidene fluoride membranes. The membranes were blocked with 5% BSA in TBST for 2 h at room temperature (RT) and subsequently incubated with primary antibodies overnight at 4 ℃. The antibodies included rabbit anti-LXRβ (1:1000, ab28479, Abcam), rabbit anti-LXRα (1:1000, 14351-1-AP, Proteintech), rabbit anti-PSD95 (1:1000, A0131, Abclonal), rabbit anti-TGFB1 (1:1000, A16640, Abclonal), rabbit anti-CD16 (1:1000, A2552, Abclonal), rabbit anti-CD32 (1:1000, A12553, Abclonal), rabbit anti-BDNF (1:1000, A11028, Abclonal), rabbit anti-SYN1 (1:1000, A17362, Abclonal), rabbit anti-Arg-1 (1:1000, A1847, Abclonal), rabbit anti-iNOS (1:1000, 18985-1-AP, Proteintech), rabbit anti-CD206 (1:1000, ab64693, Abcam), rabbit anti-GAPDH (1:2000, A19056, Abclonal), rabbit anti-Akt (1:1000, 9272, Cell signaling technology), rabbit anti-p-AKT (1:1000, 4060, Cell signaling technology), rabbit anti-PI3K (1:1000, 600225-1-Ig, Proteintech), rabbit anti-p-PI3K (1:1000, AF3241, Affinity). After washing with TBST, the membranes were incubated with a goat anti-rabbit secondary antibody (1:10000, BA1055, Boster) for 2 h at RT. The protein bands were detected by enhanced chemiluminescence (Pierce ECL Western Blotting Substrate, Thermo Scientific) and a computerized image analysis system (ChemiDoc XRS+, Bio-Rad). The intensity of bands was analyzed using Image Lab software (Bio-Rad), normalized to GAPDH, and expressed as the fold of control. The band intensity of Sham, Sham+Vehicle, or SNI+Vehicle groups in each experiment was set as 1 [37].

2.7 Enzyme-linked immunosorbent assay (ELISA)

The bilateral hippocampus was homogenized and subjected to centrifugation. The supernatants

of tissue homogenates were collected, and the levels of IL-1β, TNF-α, IL-10, and IL-4 were measured using commercially available ELISA kits (Elabscience Biotechnology, China). The procedures were conducted following the manufacturer's instructions.

2.8 Immunofluorescence

The brains were collected and postfixed in 4% paraformaldehyde (PFA) at 4 ℃ overnight. Subsequently, they were dehydrated in 20% sucrose for 24 h, followed by 30% sucrose for another 24 h. Coronal brain sections were obtained at 20 μm in thickness. The sections were blocked with 5% donkey serum and 0.3% Triton in PBS for 2 h at RT. Later, the sections were incubated overnight at 4 ℃ with the primary antibodies, including goat anti-Iba1 (1:200, ab5076, Abcam), rabbit anti-CD68 (1:500, ab125212, Abcam), anti-Arg-1 (1:100, A1847, Abclonal), rabbit anti-LXRβ (1:200, ab28479, Abcam), mouse anti-NeuN (1:500, 66836-1-lg, Proteintech), goat anti-GFAP (1:1000, ab7260, abcam), rabbit anti-Arg-1 (1:200, A1847, Abclonal). After washing with PBS, the sections were incubated with Alexa Fluor 488-labeled donkey anti-goat secondary antibody, Alexa Fluor Cy3-labeled donkey anti-rabbit secondary antibody, or Alexa Fluor 488-labeled donkey anti-mouse secondary antibody (1:500, Jackson ImmunoResearch). Nuclei were stained by DAPI for 10 min (1:5000, Beyotime). We imaged hippocampal sections using a fluorescence scanner (Olympus, Japan) and a confocal microscope (Leica, Germany) with the same exposure settings in each image set. As previously described [38,39], the mean fluorescence intensity, the number of Iba^+ cells of microglia, the number of $CD68^+$ and $Arg\text{-}1^+$ cells, and their colocalization with Iba1 staining were calculated by using Image J. Three sections per mouse were averaged and each group included 4 animals.

2.9 Statistical analysis

All data are shown as mean ± SEM. For two groups of comparison, an unpaired Student's *t*-test was applied. To analyze MPWT and four groups' data, two-way ANOVA followed by Turkey *post-hoc* test was used. The experimental data all conform to the normal distribution. GraphPad Prism 8.0 was used for all analyses. $P < 0.05$ was considered statistically significant in this study. The detailed descriptions of statistical analysis are provided in Supplementary Table 2.

3. Results

3.1 Cognitive dysfunction and hippocampal LXRβ reduction of SNI mice

As described in our previous studies, we evaluated the MPWT to assess nociceptive symptoms [40]. In the SNI group, MPWT was decreased in the ipsilateral hind paw from day 3 and persisted for at least 14 days (Fig. 1B). No difference was found in the path length (Fig. 1C) and velocity (Fig. 1D) in the OFT. Learning and memory function was then evaluated using the NORT. In the training stage, there was no difference in the total time spent exploring identical objects between the two groups (Fig. 1E). However, during the testing session, mice in the Sham group spent more time exploring the novel object than the familiar object, while SNI mice did not demonstrate a preference for the novel object (Fig. 1F-H). These findings suggest that SNI induced cognitive dysfunction in mice, but did not their alter locomotive activity.

To explore the potential role of LXRs in cognitive function in pain conditions, we detected the expression levels of LXRα and LXRβ in the hippocampus using Western blot analysis. The results indicated a significant reduction in the protein level of LXRβ in the SNI group, while there were no significant changes in the expression of LXRα following SNI (Fig. 2A). Double immunofluorescence staining revealed that LXRβ was expressed in neurons (NeuN), astrocytes (GFAP), and microglia (Iba1) in the hippocampus after SNI (Fig. 2B).

3.2 Microglia were activated and mainly expressed as M1 phenotype in the hippocampus after SNI

Neuroinflammation is an important mechanism underlying cognitive impairment. We found that microglia in the hippocampus were activated after SNI and developed into an ameboid form, with enlarged soma size and thickening processes (Fig. 3A). The quantitative results showed that the microglia-specific marker, Iba1, was highly expressed in the hippocampus after SNI (Fig. 3B-C). Besides, we also observed an increase of pro-inflammatory cytokines TNF-α, IL-1β, and a decrease of anti-inflammatory cytokines IL-10, IL-4 in the hippocampus after SNI (Fig. 3D).

Then, we used western blot and immunofluorescence to evaluate the status of microglia by examining the expression levels of markers associated with M1 and M2 phenotypes. The results indicated an elevation in the expression levels of M1 phenotype microglia markers, including CD16, CD32, and iNOS (Fig. 3E). Conversely, the levels of M2 phenotype microglial markers, such as TGF-β, Arg-1, and CD206, were reduced in the hippocampus after SNI (Fig. 3F). Furthermore, double immunofluorescent staining demonstrated a higher proportion of M1-polarized microglial marker CD68-positive microglia in the SNI group compared to Sham mice (Fig. 3G-H). In contrast, a lower proportion of M2-polarized microglial marker Arg-1-positive microglia was observed in the SNI group (Fig. 3I-J). These findings suggest that microglia were significantly activated and predominantly expressed the M1 phenotype in the hippocampus following SNI.

3.3 Decreased synaptic proteins and suppressed PI3K/AKT signaling pathway in the hippocampus after SNI

As synaptic plasticity in the hippocampus is known to be crucial for memory formation, we

assessed the levels of synaptic plasticity-related proteins. The results demonstrated a significant decrease in the expression of PSD95 (a marker for postsynaptic protein), SYN1 (a marker for presynaptic protein), and BDNF (brain-derived neurotrophic factor) after SNI (Fig. 4A). Previous studies have indicated the importance of PI3K/AKT pathway in microglia polarization and synaptic plasticity. Compared to the Sham group, the SNI group exhibited significantly lower ratios of p-PI3K/PI3K and p-AKT/AKT (Fig. 4B-C). These findings suggest that SNI led to synaptic loss and decreased activity of PI3K/AKT pathway in the hippocampus.

3.4 Activation of LXRs with T0901317 improved cognitive dysfunction induced by SNI

T0901317 is a highly selective agonist of LXRs. Our results indicated that administration of T0901317 did not affect the pain threshold (Fig. 5B), locomotion, or the exploration time of objects in mice (Supplementary Fig. 2A-C). During the testing phase of the NORT, mice in the SNI group treated with T0901317 exhibited a significant increase in the time spent on the novel object (Fig. 5C), and the discrimination ratio was also higher compared to the SNI group treated with vehicle (Fig. 5D).

3.5 T0901317 prevented the low immunocontent of LXRs and the decreased activity of PI3K/AKT signaling pathway induced by SNI

The administration of T0901317 led to an increase in the expression level of LXRβ in both the Sham and SNI groups, However, the levels of LXR-α remained unaffected by either SNI or T0901317 treatment (Fig. 5F-G). Meanwhile, the inhibited phosphorylation of PI3K and AKT proteins caused by neuropathic pain was reversed by T0901317 treatment (Fig. 5F, 5H). These results indicate that T0901317 positively impacts LXRβ expression and PI3K/AKT signaling pathway in the hippocampus, which might contribute to its beneficial effects in alleviating

cognitive dysfunction in SNI mice.

3.6 T0901317 prevented hippocampal neuroinflammation, microglial M1-polarization, and synaptic loss induced by SNI

Studies indicated that activation of LXRs alleviates microglia-mediated inflammation [33, 34]. However, research on the role of LXRs-mediated supraspinal neuroinflammation in pain is limited. Thus, the effects of T0901317 on microglia activation and inflammatory factors were measured. Iba1 staining showed that administration of T0901317 significantly alleviated the expression of Iba1 in the hippocampus after SNI (Fig. 6A-C). Moreover, T0901317 administration prevented the high levels of pro-inflammation cytokines TNF-α and IL-1β, while it upregulated anti-inflammatory factors in the hippocampus (Fig. 6D). Subsequently, we found that T0901317 reduced the expression levels of M1-phenotype markers iNOS, CD16, and CD32 and increased the levels of M2-phenotype markers CD206, TGF-β, and Arg-1 in SNI mice (Fig. 6E). Double-labelling immunofluorescence revealed that T0901317 decreased the proportion of CD68-positive microglia and increased Arg-1-positive microglia in the SNI group (Fig. 6F-I). Overall, these results collectively suggest that LXRs agonist T0901317 promoted microglial M2 polarizaiton and inhibited neuroinflammtion in the hippocampus in SNI mice.

In addition, our investigation revealed that the expression levels of PSD95, SYN1, and BDNF were significantly upregulated following T0901317 administration in both Sham and SNI groups (Fig. 6J), indicating that activation of LXRs had beneficial effects on synapse synthesis and protection.

3.7 LXRs antagonist GSK2033 blocked the neuroprotective effects of T0901317 in SNI mice

We administered LXRs antagonist GSK2033 to further confirm the roles of LXRs in cognitive

dysfunction induced by SNI. Our results showed that GSK2033 had no impact on pain behaviors (Fig. 7B) and locomotion in SNI mice (Supplementary Fig. 2D-F). However, GSK2033 completely abolished the memory protective effects of T0901317 (Fig. 7C-E). In addition, GSK2033 decreased the LXRβ expression in the SNI group and inhibited the activation of PI3K/AKT pathway induced by T0901317 (Fig. 7F-H). Furthermore, GSK2033 significantly enhanced microglia-mediated neuroinflammation (Fig. 8A-D) and reversed the microglia M2 transformation induced by T0901317 in the SNI group ((Fig. 8E-I). Moreover, GSK2033 reduced the expression levels of synaptic proteins in the SNI group and inhibited the increase of synaptic proteins after T0901317 (Fig. 8J). These findings suggest that LXRs antagonist GSK2033 exacerbated SNI-induced cognitive deficits and hippocampal dysfunction, and suppressed the neuroprotective effects of T0901317.

3.8 PI3K/AKT activation is required for the T0901317-induced neuroprotective effects

As we can conclude from the results, T0901317 reversed the suppressed activity of PI3K/AKT signaling pathway induced by neuropathic pain. We applied a specific PI3K inhibitor, LY294002, to further assess the involvement of PI3K/AKT signaling pathway underlying the neuroprotective effects of LXRs in SNI mice. LY294002 did not affect the pain behavior (Fig. 9B) and locomotion (Supplementary Fig. 2G-I), whereas significantly blocked the improvment of cognitive fucntion induced by T0901317 (Fig. 9C-E). What's more, our results showed that LY294002 aggravated hippocampal neuroinflammation (Fig. 9F-I), inhibited the transformation of microglia from M1 to M2 phenotype (Fig. 10A-E), and prevented the increased expressions of PSD95, SYN1, and BDNF induced by T0901317 (Fig. 10F). Overall, these results indicate that activation of LXRs with T0901317 alleviated the cognitive dysfunction, promoted microglia M2 polarization and

346 increased synaptic proteins in SNI mice, at least in part, through activating PI3K/AKT signaling
347 pathway.

348 **4. Discussion**

349 In the current study, we mainly investigated the effects of LXRs activation on cognitive deficits
350 caused by neuropathic pain. Our findings demonstrated that activation of LXRs with T0901317
351 improved cognitive deficits induced by SNI, promoted microglial polarization from M1 to M2,
352 inhibited inflammatory responses, and restored synaptic proteins in the hippocampus. Notably,
353 blocking LXRs or inhibiting PI3K signaling pathway reversed the beneficial effects of T0901317.
354 Finally, our findings suggest that LXRs activation has the potential to attenuate microglia-
355 mediated neuroinflammation and synaptic impairment activating the PI3K/Akt signaling pathway
356 in the hippocampus, ultimately improving pain-induced cognitive deficits (Fig. 11).

357 Pain is a complex sensory experience that affects cognition, emotion, and behavior [43]. In this
358 study, we observed that chronic neuropathic pain led to novel-object recognition dysfunction,
359 without locomotive dysfunction. This finding is in agreement with the previous findings in the
360 SNI model [15]. Moriarty et al. have proposed three theories to illustrate how pain affects
361 cognitive function: (1) limited cognitive resources; (2) altered neural plasticity; and (3)
362 unbalanced neuromediators [44]. The hippocampus, known for its role in cognition formation and
363 supraspinal modulation of pain, is considered to be the primary target affected by persistent pain
364 [45]. Neuroinflammation is an important mechanism of cognitive impairment in CNS diseases,
365 characterized by elevated pro-inflammatory cytokine and microglial activation [46]. Supraspinal
366 neuroinflammation induced by peripheral nerve injury can be initiated and maintained by the local
367 immune response in the CNS and the release of inflammatory cytokines from peripheral damaged

368 nerves [5,47]. Glia activation occurs in response to ascending pain signals at the supraspinal level
369 [48]. Additionally, the immune mediators released by damaged peripheral nerves can be relayed to
370 brain regions via ascending spinal afferents and humoral transmission across the blood-brain
371 barrier (BBB) [49]. Disrupted BBB permeability [50] and increased perivascular macrophages
372 (PVMs) in the brain [51] also contribute to pain-induced neuroinflammation in the hippocampus.
373 Studies have demonstrated the overexpression of pro-inflammatory cytokines, including TNF-α,
374 IL-1β, and IL-6, in the hippocampus, plasma, and cerebrospinal fluid in pain models [6,52–54].

375 Reactive microglia can alter and adapt to neurotoxic (M1) and neuroprotective phenotype (M2).
376 M1 microglia can be stimulated by pro-inflammatory factors and are characterized by increased
377 expression of several proteins or inflammatory cytokines, such as iNOS, CD68, CD16/32, IL-1β,
378 and TNF-α. Conversely, M2 microglia can be induced by IL-4 and IL-10 and exhibit increased
379 expression of Arg-1, CD206 or anti-inflammation cytokines IL-4 and IL-10 [55]. In our study, we
380 observed an exaggerated activation of microglia, along with increased levels of TNF-α and IL-1β,
381 and reduced levels of IL-4 and IL-10 in the hippocampus after SNI. The results further suggest
382 that SNI-induced cognitive dysfunction was associated with microglial M1 polarization in the
383 hippocampus, as demonstrated by increased M1 marker expression and decreased M2 marker
384 expression, which supports the neuromediator theory. It has been demonstrated that modulating
385 M1/M2 polarization is beneficial for regulating neural homeostasis and improving behavioral
386 outcomes. However, Kwon and Koh suggested that the traditional category of microglia
387 polarization (M1/M2) should be considered as a spectrum rather than two different populations
388 [56]. To better understand microglial diversities in neurological diseases, some unbiased
389 approaches such as transcriptomics are expected to be employed in future research [57].

Synapse plasticity impairment is characteristic of many neurological pathologies associated with neuroinflammation, such as AD [58] and depression [59]. In this study, we found that SNI significantly decreased the expression levels of synaptic-related proteins, including PSD95, SYN1, and BDNF. These results are consistent with our previous findings that SNI impaired hippocampal synaptic plasticity in rats, as demonstrated by deficient long-time potential (LTP) and reduced excitatory synapses [60]. Morphological research also showed that SNI reduced spine density and dendrite tree complexity of hippocampal pyramidal neurons [16]. Moreover, Liu et al highlighted that TNF-α signaling and microglial activation induced by SNI disrupts synaptic structural and functional plasticity in the hippocampus [10]. Recent studies have also indicated that the deregulated engulfment of synaptic structures by activated microglia contributes to synapse loss in the hippocampus and cognitive decline [61, 62].

LXRs are activated by endogenous cholesterol derivatives like oxysterols, and they regulate gene transcription involved in cholesterol metabolism and immunomodulation across various cell types [22]. Here, we found that LXRβ was decreased in the hippocampus at 14 days after SNI, which is in line with similar research on cognitive impairment [26]. In the mature brain, cholesterol is primarily produced by astrocytes and neural stem cells. However, it has been reported that persistent pain leads to poor neurogenesis [63] and astrocyte atrophy [64] in the hippocampus, which may contribute to insufficient cholesterol synthesis. Consequently, the reduction in hippocampal LXRβ expression induced by SNI may be associated with inadequate cholesterol signaling produced during the pain condition in the hippocampus.

Our study showed that LXRs synthetic agonist T0901317 increased LXRβ expression and significantly improved cognitive dysfunction in SNI mice. Immunofluorescence staining revealed

412 that LXRβ was widely expressed in neurons, astrocytes, and microglia following SNI. In this
413 study, we primarily focused on exploring the effects of LXRs on microglia-mediated
414 neuroinflammation and neuronal synapse loss. Firstly, we observed that LXRs activation
415 effectively inhibted microglia activation, promoted microglia polarization from M1 to the M2
416 phenotype, and decreased the levels of pro-inflammtory cytokines in the hippocampus after SNI.
417 Previous studies have reported that LXRs downregulate proinflammatory gene expression in the
418 activated microglia, including nuclear factor-kappa B (NF-κB), resulting in reduced release of
419 iNOS and IL-1β, and promoting the transition to M2 states of microglia [65]. Additionally, Zhang
420 et al. found that GW3965 reduced cholesterol burden in the phagocytes, facilitating the
421 transformation of proinflammatory microglia into neuroprotective ones in mice with brain injury
422 [66]. Moreover, LXRs are the key modulator of cholesterol which is the essential material for
423 synapse formation, axon growth, and membrane homeostasis [67]. Our results showed that
424 administration of T0901317 significantly increased synaptic proteins in the Sham and SNI groups.
425 Xu et al. also demonstrated that GW3965 prevents the disruption of LTP and the reduction in
426 spine density induced by chronic stress [27]. These results highlighted the beneficial role of LXRs
427 in the formation and restoration of synaptic plasticity. To further confirm the effects of T0901317
428 in the CNS, we microinjected LXR antagonist GSK2033 into the lateral ventricle. The results
429 showed that the neuroprotective effects of T0901317 were completely countervailed by GSK2033.
430 As to the pain behavior, it has been reported that activation of LXRs inhibited hyperalgesia in
431 CFA-induced inflammatory pain [68]. However, in this study, treatment with T0901317 or
432 GSK2033 did not affect the pain behaviors of SNI mice. The differences in analgesic effects of
433 LXRs could be attributed to variations in animal pain models and drug delivery methods.

In the peripheral system, downregulation of LXR/PI3K/AKT pathway can inhibit M2 macrophage formation and attenuate renal fibrosis [69]. In the CNS, Akt regulated M2 microglial polarization via Ser473 phosphorylation in brain diseases [70,71]. Moreover, PI3K/AKT signaling pathway also plays a key role in synaptic plasticity. For example, T0901317 significantly restored synapses in the ischemic brain by increasing PI3K/Akt signaling [29]. Insulin signaling regulates dendritic spine formation and excitatory synapse development in hippocampal neurons through the activation of PI3K/Akt/mTOR pathways [72]. Our findings indicate that PI3K/AKT signaling pathway was inhibited in the hippocampus after SNI, accompanied by microglia M1 polarization and impairment of synaptic plasticity. However, activation of LXRs by T0901317 significantly reversed the suppressed PI3K/AKT signaling pathway induced by SNI. Furthermore, PI3K inhibitor LY294002 exacerbated the cognitive dysfunction in SNI mice and abolished the neuroprotective effects of T0901317. In summary, our results suggest that activation of PI3K/AKT signaling pathway is a major contributor to the LXRs-mediated microglia polarization and synaptic plasticity.

There were limitations to our study. Firstly, we focused on SNI-induced neuroinflammation and synaptic impairment in the hippocampus and did not examine other cognition-related brain regions. Secondly, since the gene knockout technology can effectively distinguish the functions of different subunits, we could have used knockout mice to further verify the functions of LXR α/β. Lastly, our study reported that LXRs can regulate microglia polarization and synaptic proteins, but further research is required to investigate the specific expression and functional changes of LXRs in different cell types within the brain and their association with cognitive function.

In summary, our study reveals the impact of LXRs on cognitive dysfunction induced by

neuropathic pain. We found that neuropathic pain disrupted cognitive function and LXRs expression in the hippocampus. Activation of LXRs with T0901317 attenuated pain-induced cognitive dysfunction by modulating microglia polarization, neuroinflammation, and synaptic plasticity in the hippocampus through the activation of PI3K/AKT signaling pathway. Thus, LXRs could be a potential target to prevent or treat patients who suffer from pain-induced cognitive disorders.

References:

1. Mills SEE, Nicolson KP, Smith BH. Chronic pain: a review of its epidemiology and associated factors in population-based studies. British Journal of Anaesthesia. 2019;123:e273–83.

2. Phelps CE, Navratilova E, Porreca F. Cognition in the Chronic Pain Experience: Preclinical Insights. Trends in Cognitive Sciences. 2021;25:365–76.

3. Zhao W, Zhao L, Chang X, Lu X, Tu Y. Elevated dementia risk, cognitive decline, and hippocampal atrophy in multisite chronic pain. Proc Natl Acad Sci USA. 2023;120:e2215192120.

4. Low LA. The impact of pain upon cognition: what have rodent studies told us? Pain. 2013;154:2603–5.

5. Fiore NT, Austin PJ. Are the emergence of affective disturbances in neuropathic pain states contingent on supraspinal neuroinflammation? Brain, Behavior, and Immunity. 2016;56:397–411.

6. Ren W-J, Liu Y, Zhou L-J, Li W, Zhong Y, Pang R-P, et al. Peripheral nerve injury leads to working memory deficits and dysfunction of the hippocampus by upregulation of TNF-α in

476 rodents. Neuropsychopharmacology. 2011;36:979–92.

477 7. Gui W-S, Wei X, Mai C-L, Murugan M, Wu L-J, Xin W-J, et al. Interleukin-1β overproduction
478 is a common cause for neuropathic pain, memory deficit, and depression following peripheral
479 nerve injury in rodents. Mol Pain. 2016;12:174480691664678.

480 8. Saffarpour S, Janzadeh A, Rahimi B, Ramezani F, Nasirinezhad F. Chronic nanocurcumin
481 treatment ameliorates pain-related behavior, improves spatial memory, and reduces hippocampal
482 levels of IL-1β and TNFα in the chronic constriction injury model of neuropathic pain.
483 Psychopharmacology. 2021;238:877–86.

484 9. Vasic V, Schmidt M. Resilience and Vulnerability to Pain and Inflammation in the
485 Hippocampus. IJMS. 2017;18:739.

486 10. Liu Y, Zhou L-J, Wang J, Li D, Ren W-J, Peng J, et al. TNF-α Differentially Regulates
487 Synaptic Plasticity in the Hippocampus and Spinal Cord by Microglia-Dependent Mechanisms
488 after Peripheral Nerve Injury. The Journal of Neuroscience. 2017;37:871–81.

489 11. Wang Y, Leak RK, Cao G. Microglia-mediated neuroinflammation and neuroplasticity after
490 stroke. Front Cell Neurosci. 2022;16:980722.

491 12. Cornell J, Salinas S, Huang H-Y, Zhou M. Microglia regulation of synaptic plasticity and
492 learning and memory. Neural Regen Res. 2021;17:705–16.

493 13. Lecca D, Jung YJ, Scerba MT, Hwang I, Kim YK, Kim S, et al. Role of chronic
494 neuroinflammation in neuroplasticity and cognitive function: A hypothesis. Alzheimers Dement.

2022;18:2327–40.

14. Hisaoka-Nakashima K, Ohata K, Yoshimoto N, Tokuda S, Yoshii N, Nakamura Y, et al. High-mobility group box 1-mediated hippocampal microglial activation induces cognitive impairment in mice with neuropathic pain. Experimental Neurology. 2022;355:114146.

15. Guida F, Iannotta M, Misso G, Ricciardi F, Boccella S, Tirino V, et al. Long-term neuropathic pain behaviors correlate with synaptic plasticity and limbic circuit alteration: a comparative observational study in mice. Pain. 2022;163:1590–602.

16. Tyrtyshnaia A, Manzhulo I. Neuropathic Pain Causes Memory Deficits and Dendrite Tree Morphology Changes in Mouse Hippocampus. Journal of Pain Research. 2020;13:345–54.

17. Mutso AA, Radzicki D, Baliki MN, Huang L, Banisadr G, Centeno MV, et al. Abnormalities in Hippocampal Functioning with Persistent Pain. J Neurosci. 2012;32:5747–56.

18. Tyrtyshnaia A, Bondar A, Konovalova S, Manzhulo I. Synaptamide Improves Cognitive Functions and Neuronal Plasticity in Neuropathic Pain. Int J Mol Sci. 2021;22:12779.

19. Moutinho M, Codocedo JF, Puntambekar SS, Landreth GE. Nuclear Receptors as Therapeutic Targets for Neurodegenerative Diseases: Lost in Translation. Annual Review of Pharmacology and Toxicology. 2019;59:237–61.

20. Fitz NF, Nam KN, Koldamova R, Lefterov I. Therapeutic targeting of nuclear receptors, liver X and retinoid X receptors, for Alzheimer's disease. Br J Pharmacol. 2019;176:3599–610.

21. Xu P, Li D, Tang X, Bao X, Huang J, Tang Y, et al. LXR agonists: new potential therapeutic

514 drug for neurodegenerative diseases. Mol Neurobiol. 2013;48:715–28.

515 22. Wang B, Tontonoz P. Liver X receptors in lipid signalling and membrane homeostasis. Nat
516 Rev Endocrinol. 2018;14:452–63.

517 23. Loane DJ, Washington PM, Vardanian L, Pocivavsek A, Hoe H-S, Duff KE, et al. Modulation
518 of ABCA1 by an LXR agonist reduces β-amyloid levels and improves outcome after traumatic
519 brain injury. J Neurotrauma. 2011;28:225–36.

520 24. Dai J, Xu S, Okada T, Liu Y, Zuo G, Tang J, et al. T0901317, an Agonist of Liver X Receptors,
521 Attenuates Neuronal Apoptosis in Early Brain Injury after Subarachnoid Hemorrhage in Rats via
522 Liver X Receptors/Interferon Regulatory Factor/P53 Upregulated Modulator of
523 Apoptosis/Dynamin-1-Like Protein Pathway. Gebicki J, editor. Oxidative Medicine and Cellular
524 Longevity. 2021;2021:1–16.

525 25. Repa JJ, Li H, Frank-Cannon TC, Valasek MA, Turley SD, Tansey MG, et al. Liver X
526 Receptor Activation Enhances Cholesterol Loss from the Brain, Decreases Neuroinflammation,
527 and Increases Survival of the NPC1 Mouse. J Neurosci. 2007;27:14470–80.

528 26. Qiu C, Wang M, Yu W, Rong Z, Zheng H-S, Sun T, et al. Activation of the Hippocampal
529 LXRβ Improves Sleep-Deprived Cognitive Impairment by Inhibiting Neuroinflammation. Mol
530 Neurobiol. 2021;58:5272–88.

531 27. Xu X, Xiao X, Yan Y, Zhang T. Activation of liver X receptors prevents emotional and
532 cognitive dysfunction by suppressing microglial M1-polarization and restoring synaptic plasticity

533 in the hippocampus of mice. Brain Behav Immun. 2021;94:111–24.

534 28. Sun T, Li YJ, Tian QQ, Wu Q, Feng D, Xue Z, et al. Activation of liver X receptor beta-
535 enhancing neurogenesis ameliorates cognitive impairment induced by chronic cerebral
536 hypoperfusion. Exp Neurol. 2018;304:21–9.

537 29. Chen J, Zacharek A, Cui X, Shehadah A, Jiang H, Roberts C, et al. Treatment of stroke with a
538 synthetic liver X receptor agonist, TO901317, promotes synaptic plasticity and axonal
539 regeneration in mice. J Cereb Blood Flow Metab. 2010;30:102–9.

540 30. Cianciulli A, Porro C, Calvello R, Trotta T, Lofrumento DD, Panaro MA. Microglia Mediated
541 Neuroinflammation: Focus on PI3K Modulation. Biomolecules. 2020;10:137.

542 31. Wang Y, Lin Y, Wang L, Zhan H, Luo X, Zeng Y, et al. TREM2 ameliorates
543 neuroinflammatory response and cognitive impairment via PI3K/AKT/FoxO3a signaling pathway
544 in Alzheimer's disease mice. Aging (Albany NY). 2020;12:20862–79.

545 32. Han X, Cheng X, Xu J, Liu Y, Zhou J, Jiang L, et al. Activation of TREM2 attenuates
546 neuroinflammation via PI3K/Akt signaling pathway to improve postoperative cognitive
547 dysfunction in mice. Neuropharmacology. 2022;219:109231.

548 33. Chen L, Song D, Chen B, Yang X, Cheng O. Activation of liver X receptor promotes
549 hippocampal neurogenesis and improves long-term cognitive function recovery in acute cerebral
550 ischemia-reperfusion mice. J Neurochem. 2020;154:205–17.

551 34. Lu L, Liu X, Fu J, Liang J, Hou Y, Dou H. sTREM-1 promotes the phagocytic function of

552 microglia to induce hippocampus damage via the PI3K–AKT signaling pathway. Sci Rep.
553 2022;12:7047.

554 35. Zhang W, Xiong BR, Zhang LQ, Huang X, Zhou WC, Zou Q, et al. Disruption of the
555 GABAergic system contributes to the development of perioperative neurocognitive disorders after
556 anesthesia and surgery in aged mice. CNS Neurosci Ther. 2020;26:913–24.

557 36. Xiao JY, Xiong BR, Zhang W, Zhou WC, Yang H, Gao F, et al. PGE2-EP3 signaling
558 exacerbates hippocampus-dependent cognitive impairment after laparotomy by reducing
559 expression levels of hippocampal synaptic plasticity-related proteins in aged mice. CNS Neurosci
560 Ther. 2018;24:917–29.

561 37. Zhang L-Q, Gao S-J, Sun J, Li D-Y, Wu J-Y, Song F-H, et al. DKK3 ameliorates neuropathic
562 pain via inhibiting ASK-1/JNK/p-38-mediated microglia polarization and neuroinflammation. J
563 Neuroinflammation. 2022;19:129.

564 38. Wu H, Zheng J, Xu S, Fang Y, Wu Y, Zeng J, et al. Mer regulates microglial/macrophage
565 M1/M2 polarization and alleviates neuroinflammation following traumatic brain injury. J
566 Neuroinflammation. 2021;18:2.

567 39. Yuan X, Han S, Manyande A, Gao F, Wang J, Zhang W, et al. Spinal voltage-gated potassium
568 channel Kv1.3 contributes to neuropathic pain via the promotion of microglial M1 polarization
569 and activation of the NLRP3 inflammasome. European Journal of Pain. 2023;27:289–302.

570 40. Zhang LQ, Zhang W, Li T, Yang T, Yuan X, Zhou Y, et al. GLP-1R activation ameliorated

571 novel-object recognition memory dysfunction via regulating hippocampal AMPK/NF-kappaB
572 pathway in neuropathic pain mice. Neurobiol Learn Mem. 2021;182:107463.

573 41. Li J, Zhu P, Li Y, Xiao K, Tang J, Liang X, et al. The liver X receptors agonist GW3965
574 attenuates depressive-like behaviors and suppresses microglial activation and neuroinflammation
575 in hippocampal subregions in a mouse depression model. J of Comparative Neurology.
576 2022;530:2852–67.

577 42. Zhang-Gandhi CX, Drew PD. Liver X receptor and retinoid X receptor agonists inhibit
578 inflammatory responses of microglia and astrocytes. J Neuroimmunol. 2007;183:50–9.

579 43. Liu M-G, Chen J. Preclinical research on pain comorbidity with affective disorders and
580 cognitive deficits: Challenges and perspectives. Progress in Neurobiology. 2014;116:13–32.

581 44. Moriarty O, McGuire BE, Finn DP. The effect of pain on cognitive function: a review of
582 clinical and preclinical research. Prog Neurobiol. 2011;93:385–404.

583 45. McCarberg B, Peppin J. Pain Pathways and Nervous System Plasticity: Learning and Memory
584 in Pain. Pain Medicine. 2019;20:2421–37.

585 46. Woodburn SC, Bollinger JL, Wohleb ES. The semantics of microglia activation:
586 neuroinflammation, homeostasis, and stress. J Neuroinflammation. 2021;18:258.

587 47. Liu X-G. Normalization of Neuroinflammation: A New Strategy for Treatment of Persistent
588 Pain and Memory/Emotional Deficits in Chronic Pain. JIR. 2022;Volume 15:5201–33.

589 48. Torta R, Ieraci V, Zizzi F. A Review of the Emotional Aspects of Neuropathic Pain: From

590 Comorbidity to Co-Pathogenesis. Pain Ther. 2017;6:11–7.

591 49. Austin PJ, Fiore NT. Supraspinal neuroimmune crosstalk in chronic pain states. Current
592 Opinion in Physiology. 2019;11:7–15.

593 50. Brooks TA, Hawkins BT, Huber JD, Egleton RD, Davis TP. Chronic inflammatory pain leads
594 to increased blood-brain barrier permeability and tight junction protein alterations. American
595 Journal of Physiology-Heart and Circulatory Physiology. 2005;289:H738–43.

596 51. Mai CL, Tan Z, Xu YN, Zhang JJ, Huang ZH, Wang D, et al. CXCL12-mediated monocyte
597 transmigration into brain perivascular space leads to neuroinflammation and memory deficit in
598 neuropathic pain. Theranostics. 2021;11:1059–78.

599 52. Ding X, Gao X, Wang Z, Jiang X, Lu S, Xu J, et al. Preoperative Chronic and Acute Pain
600 Affects Postoperative Cognitive Function Mediated by Neurotransmitters. J Mol Neurosci.
601 2021;71:515–26.

602 53. Hisaoka-Nakashima K, Moriwaki K, Yoshimoto N, Yoshii T, Nakamura Y, Ago Y, et al. Anti-
603 interleukin-6 receptor antibody improves allodynia and cognitive impairment in mice with
604 neuropathic pain following partial sciatic nerve ligation. Int Immunopharmacol. 2022;112:109219.

605 54. del Rey A, Yau H-J, Randolf A, Centeno MV, Wildmann J, Martina M, et al. Chronic
606 neuropathic pain-like behavior correlates with IL-1β expression and disrupts cytokine interactions
607 in the hippocampus. PAIN. 2011;152:2827–35.

608 55. Wang X, Jiang Y, Li J, Wang Y, Tian Y, Guo Q, et al. DUSP1 Promotes Microglial Polarization

609 toward M2 Phenotype in the Medial Prefrontal Cortex of Neuropathic Pain Rats via Inhibition of
610 MAPK Pathway. ACS Chem Neurosci. 2021;12:966–78.

611 56. Kwon HS, Koh S-H. Neuroinflammation in neurodegenerative disorders: the roles of
612 microglia and astrocytes. Transl Neurodegener. 2020;9:42.

613 57. Ransohoff RM. A polarizing question: do M1 and M2 microglia exist? Nat Neurosci.
614 2016;19:987–91.

615 58. Tampellini D, Capetillo-Zarate E, Dumont M, Huang Z, Yu F, Lin MT, et al. Effects of
616 Synaptic Modulation on β-Amyloid, Synaptophysin, and Memory Performance in Alzheimer's
617 Disease Transgenic Mice. J Neurosci. 2010;30:14299–304.

618 59. Wang J, Chen H-S, Li H-H, Wang H-J, Zou R-S, Lu X-J, et al. Microglia-dependent excessive
619 synaptic pruning leads to cortical underconnectivity and behavioral abnormality following chronic
620 social defeat stress in mice. Brain, Behavior, and Immunity. 2023;109:23–36.

621 60. Xiong B, Zhang W, Zhang L, Huang X, Zhou W, Zou Q, et al. Hippocampal glutamatergic
622 synapses impairment mediated novel-object recognition dysfunction in rats with neuropathic pain.
623 Pain. 2020;161:1824–36.

624 61. Zhai Q, Zhang Y, Ye M, Zhu S, Sun J, Wang Y, et al. Reducing complement activation during
625 sleep deprivation yields cognitive improvement by dexmedetomidine. British Journal of
626 Anaesthesia. 2023;131:542–55.

627 62. Xu F, Han L, Wang Y, Deng D, Ding Y, Zhao S, et al. Prolonged anesthesia induces

neuroinflammation and complement-mediated microglial synaptic elimination involved in neurocognitive dysfunction and anxiety-like behaviors. BMC Med. 2023;21:7.

63. Egorova E, Starinets A, Tyrtyshnaia A, Ponomarenko A, Manzhulo I. Hippocampal Neurogenesis in Conditions of Chronic Stress Induced by Sciatic Nerve Injury in the Rat. Cells Tissues Organs. 2019;207:58–68.

64. Fiore NT, Austin PJ. Glial-cytokine-neuronal Adaptations in the Ventral Hippocampus of Rats with Affective Behavioral Changes Following Peripheral Nerve Injury. Neuroscience. 2018;390:119–40.

65. Bensinger SJ, Tontonoz P. Integration of metabolism and inflammation by lipid-activated nuclear receptors. Nature. 2008;454:470–7.

66. Zhang R, Dong Y, Liu Y, Moezzi D, Ghorbani S, Mirzaei R, et al. Enhanced liver X receptor signalling reduces brain injury and promotes tissue regeneration following experimental intracerebral haemorrhage: roles of microglia/macrophages. Stroke Vasc Neurol. 2023;svn-2023-002331.

67. Pfrieger FW. Role of cholesterol in synapse formation and function. Biochim Biophys Acta. 2003;1610:271–80.

68. Li YJ, Zhang K, Sun T, Wang J, Guo YY, Yang L, et al. Epigenetic suppression of liver X receptor beta in anterior cingulate cortex by HDAC5 drives CFA-induced chronic inflammatory pain. J Neuroinflammation. 2019;16:132.

69. Li X, Huang X, Feng Y, Wang Y, Guan J, Deng B, et al. Cylindrin from Imperata cylindrica inhibits M2 macrophage formation and attenuates renal fibrosis by downregulating the LXR-α/PI3K/AKT pathway. European Journal of Pharmacology. 2023;950:175771.

70. Peng J, Pang J, Huang L, Enkhjargal B, Zhang T, Mo J, et al. LRP1 activation attenuates white matter injury by modulating microglial polarization through Shc1/PI3K/Akt pathway after subarachnoid hemorrhage in rats. Redox Biology. 2019;21:101121.

71. Wang G, Shi Y, Jiang X, Leak RK, Hu X, Wu Y, et al. HDAC inhibition prevents white matter injury by modulating microglia/macrophage polarization through the GSK3β/PTEN/Akt axis. Proc Natl Acad Sci USA. 2015;112:2853–8.

72. Lee C-C, Huang C-C, Hsu K-S. Insulin promotes dendritic spine and synapse formation by the PI3K/Akt/mTOR and Rac1 signaling pathways. Neuropharmacology. 2011;61:867–79.

Figure legends:

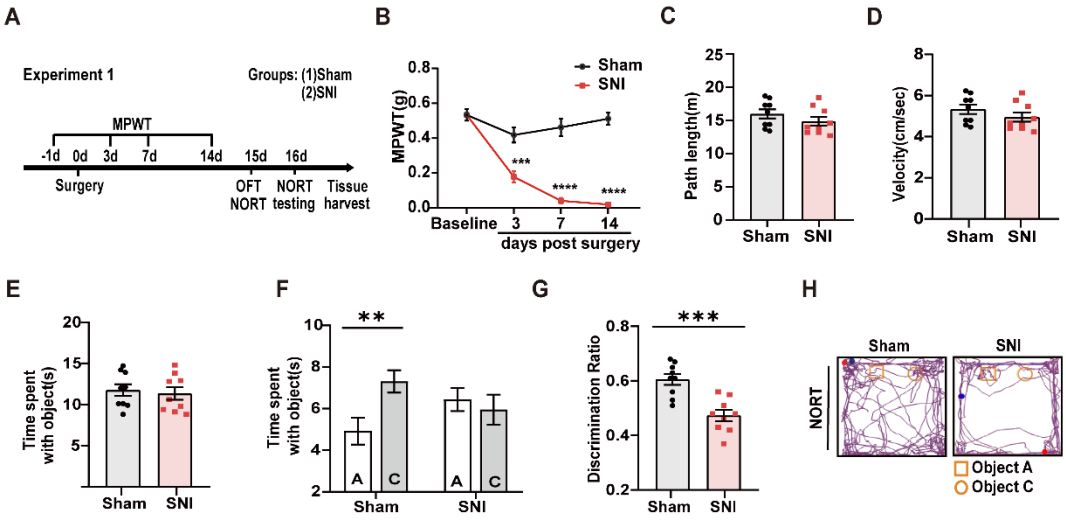

Fig. 1 The locomotive and cognitive performance after SNI

(A) Experimental designs of the Sham and SNI groups. (B) Mechanical allodynia was evaluated by the ipsilateral mechanical paw withdrawal threshold (MPWT) at 1 day before surgery and 3, 7, 14 days after surgery (compared to the corresponding day of the Sham group) (n = 9). (C-D) Path length and velocity in the OFT (n = 9). (E) Total time spent with two similar objects in the training phase of NORT (n = 9). (F) Time spent with familiar object A and novel object C in the testing phase (n = 9). (G) Discrimination ratio in the testing phase of NORT (n = 9). (H) Representative exploration traces of Sham and SNI mice in the NORT. All data are presented as mean ± SEM. Student's *t*-test; two-way ANOVA, followed by Turkey *post-hoc* test. **P < 0.05, ***P* < 0.01, ****P* < 0.001, *****P* < 0.0001, n = 9 per group. SNI: spared nerve injured; MPWT: mechanical paw withdrawal threshold; NORT: novel object recognition test; OFT: open field test.

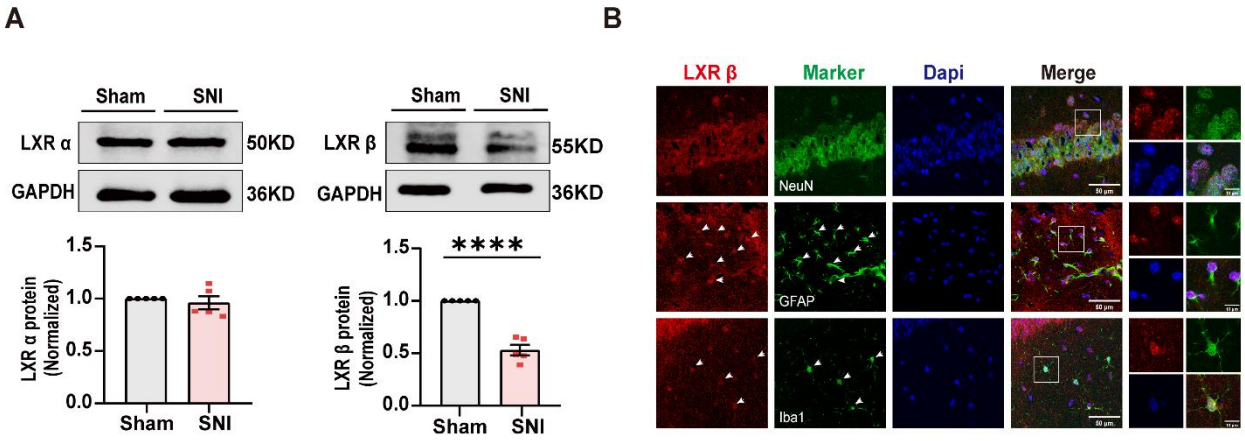

673

674 **Fig. 2 Expression profile of LXRs in the hippocampus after SNI**

675 **(A)** Representative western blot images and quantification of protein levels of LXRα and LXRβ in

676 the hippocampus of Sham and SNI mice (n = 5). (B) Representative images of colocalization of

677 LXR β (red) with neurons (NeuN, green), astrocytes (GFAP, green), and microglia (Iba1, green) in

678 the hippocampus after SNI (n = 3). Nuclei were stained with Dapi (blue). Scale bar: 50 μm and 10

679 μm for detail. All data are presented as mean ± SEM. Student's *t*-test, ****$P < 0.0001$, n = 5 per

680 group.

681

682

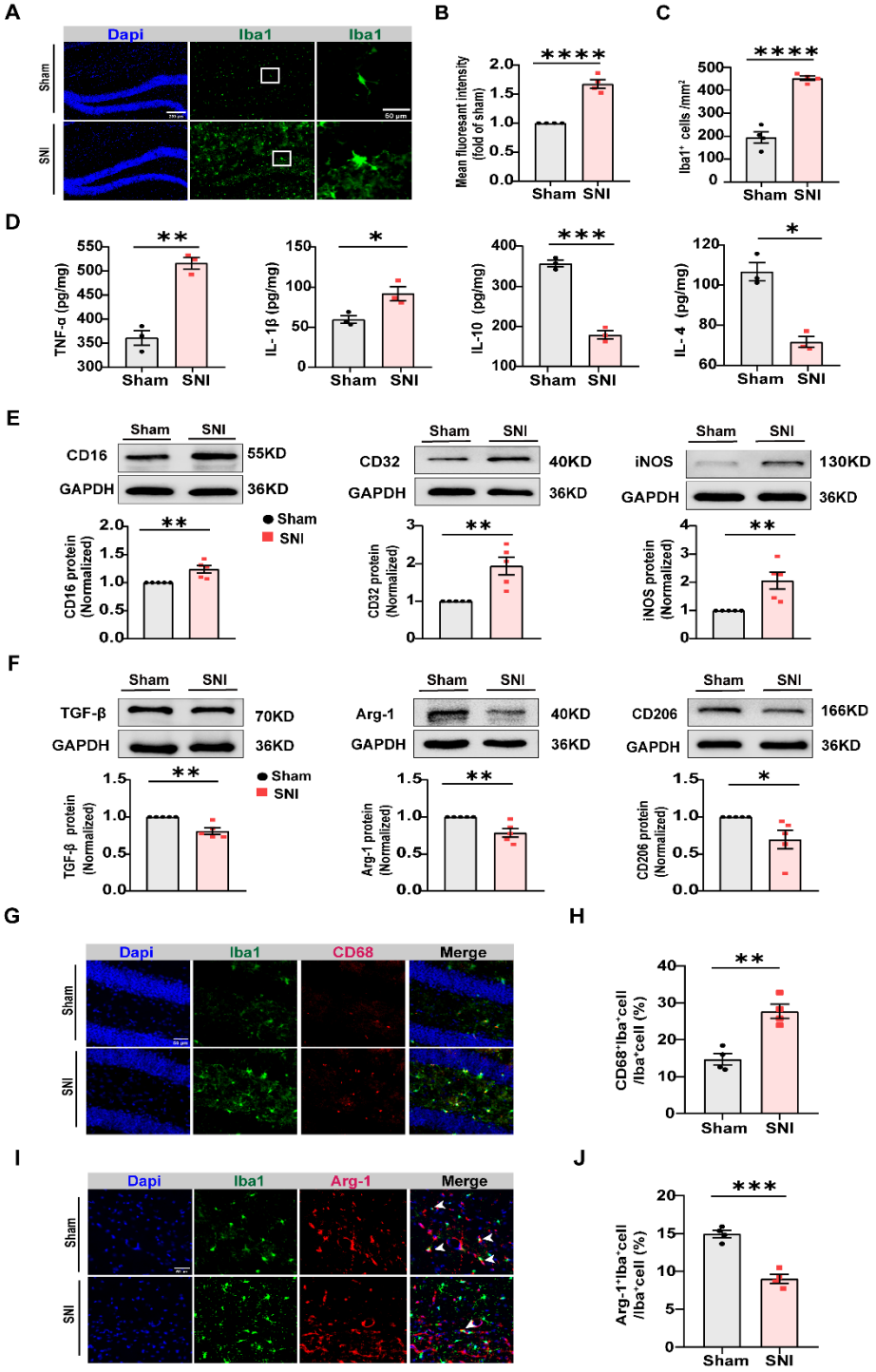

683

684 **Fig. 3 SNI induced neuroinflammation and M1 microglia polarization in the hippocampus**

685 (A) Representative images of immunofluorescence staining with Iba1 in the hippocampus sections

686 of the Sham and SNI mice. Nuclei were stained with Dapi. Scale bar: 200 μm and 50 μm, for

687 detail. (B) Quantification of the mean fluorescent intensity of Iba1-positive cells in the

hippocampus (n = 4). (C) Quantification of the number of Iba1-positive cells per square millimeter in the hippocampus (n = 4). (D) Measurement of the levels of pro-inflammatory cytokines TNF-α, IL-1β, and anti-inflammatory cytokines IL-10, IL-4 in the hippocampus (n = 3). (E) Representative western blot images and quantification of expression levels of M1 microglia markers, including CD16, CD32, and iNOS in the hippocampus of the Sham and SNI groups (n = 5). (F) Representative western blot images and quantification of expression levels of M2 microglia markers, including TGF-β, Arg-1, and CD206 in the hippocampus of the Sham and SNI groups (n = 5). (G) Double immunofluorescence staining of microglia (Iba1, green) with M1 marker (CD68, red) in the hippocampus. Nuclei were stained with Dapi. Scale bar: 50 μm. (H) Quantification of the percentage of CD68 and Iba1 double-positive cells in the hippocampus (n = 4). (I) Double immunofluorescence staining of microglia (Iba1. green) with M2 marker (Arg-1, red) in the hippocampus. Nuclei were stained with Dapi. Scale bar: 50 μm. (J) Quantification of the percentage of Arg-1 and Iba1 double-positive cells in the hippocampus (n = 4). All data are presented as mean ± SEM. Student's *t*-test. **P* < 0.05, ***P* < 0.01, ****P* < 0.001, *****P* < 0.0001, n = 3-5 per group.

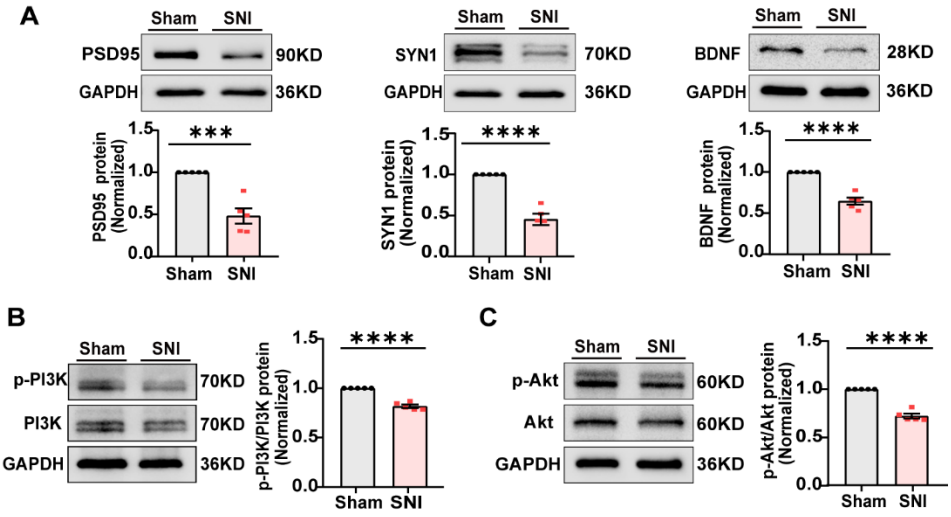

704

705 **Fig. 4 SNI decreased synaptic plasticity-related proteins and suppressed the PI3K/AKT**

706 **signaling pathway**

707 (A) Representative western blot images and quantification for synaptic proteins including PSD95,

708 SYN1, and BDNF in the hippocampus (n = 5). (B) Representative western blot images of p-PI3K

709 and PI3K expression levels and quantification for the ratio of p-PI3K/PI3K (n = 5). (C)

710 Representative western blot images of p-AKT and AKT expression levels and quantification for

711 the ratio of p-AKT/AKT (n = 5). All data are presented as mean ± SEM. Student's *t* test. ***P <

712 0.001, ****P < 0.0001, n = 5 per group.

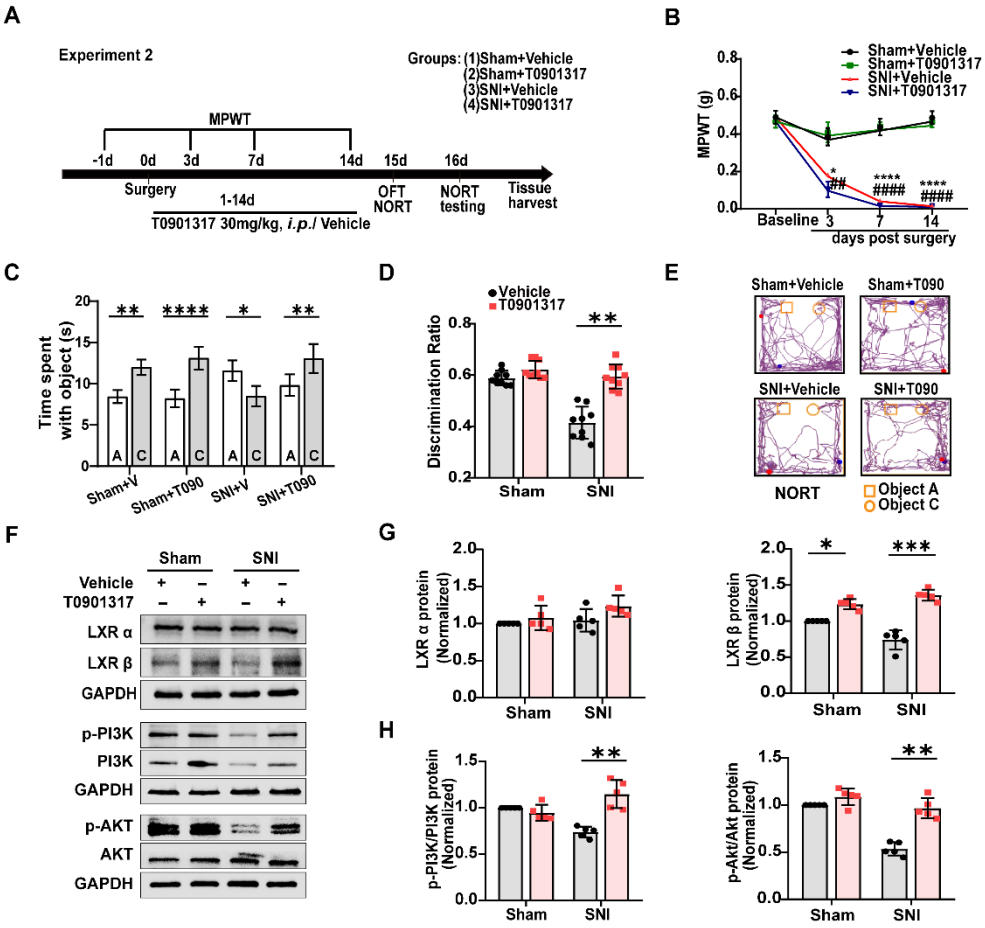

Fig. 5 LXRs agonist T0901317 effectively improved the cognitive dysfunction of SNI mice

(A) Experimental designs and animal groups in administration of LXRs agonist T0901317 (30 mg/kg, *i.p.*). (B) Mechanical allodynia was evaluated by MPWT (n = 9). (C) Time spent with familiar object A and novel object C after administration of T0901317 (n = 9). (D) Discrimination ratio in NORT testing phase (n = 9). (E) Representative exploration traces in the NORT. (F-H) Representative western blot images and quantification of expression levels of LXRs (LXRα and LXRβ) and PI3K/AKT pathway related-proteins in the hippocampus after administration of T0901317 (n = 5). All data are presented as mean ± SEM. Two-way ANOVA, followed by Turkey *post-hoc* test. *$P < 0.05$, **$P < 0.01$,***$P < 0.001$, ****$P < 0.0001$, ##$P < 0.01$, ###$P < 0.001$, ####$P < 0.0001$, n = 5-9 per group. V: Vehicle. T090: T0901317.

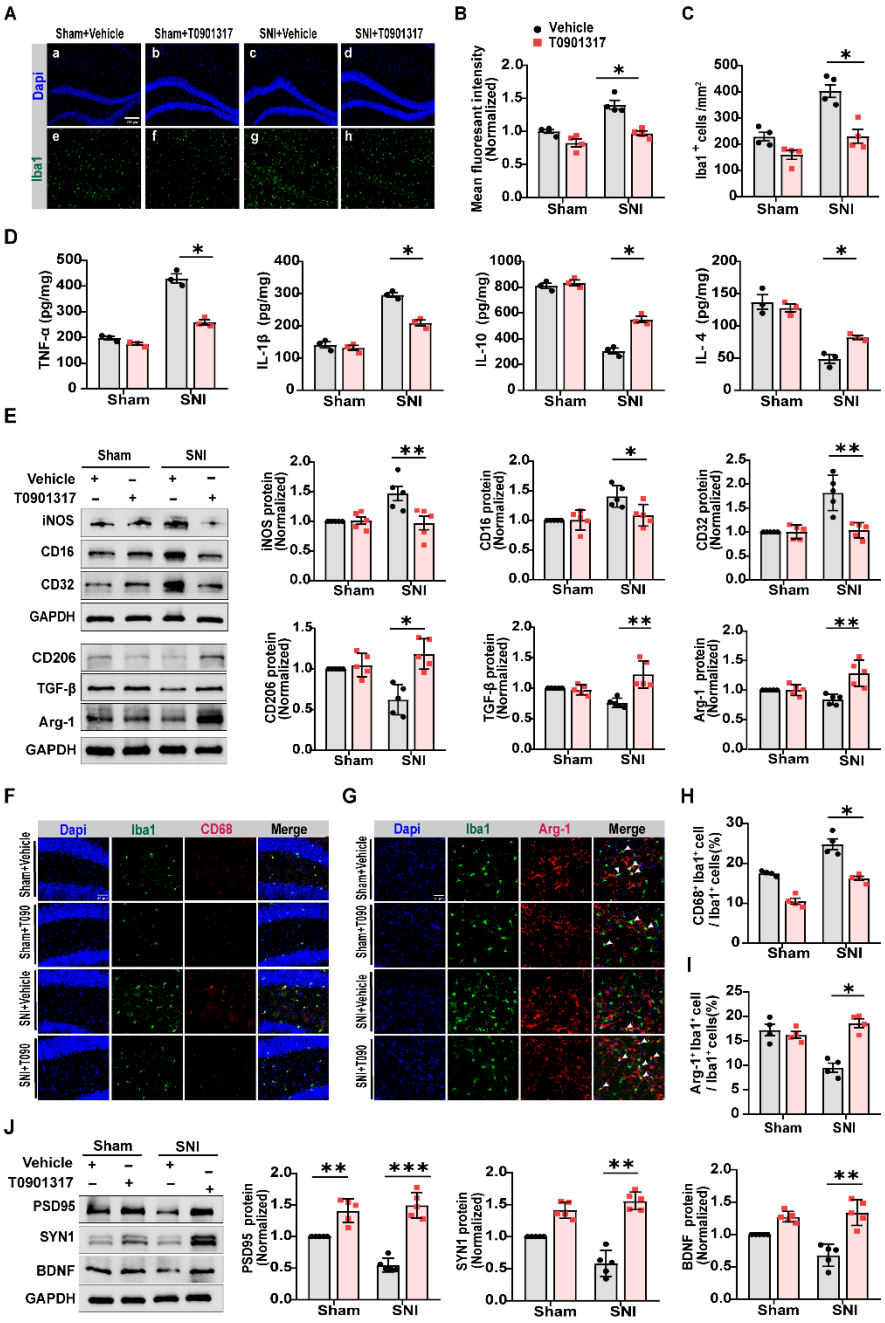

724

725 **Fig. 6 Effects of LXRs agonist T0901317 on hippocampal neuroinflammation, microglia**

726 **polarization, and synaptic plasticity in SNI mice**

727 (A) Representative images of immunofluorescence staining with Iba1 in the hippocampus sections

728 after using T0901317. Nuclei were stained with Dapi. Scale bar: 200 μm. (B) Quantification of the

729 mean fluorescent intensity of Iba1-positive cells in the hippocampus (n = 4). (C) Quantification of

730 the number of Iba1-positive cells per square millimeter in the hippocampus (n = 4). (D)
731 Measurement of the levels of pro-inflammatory cytokines TNF-α, IL-1β, and anti-inflammatory
732 cytokines IL-10, IL-4 in the hippocampus after T0901317 treatment (n = 3). (E) Representative
733 western blot images and quantification for expression levels of M1 microglia markers iNOS,
734 CD16, CD32, and M2 markers CD206, TGF-β, Arg-1 in the hippocampus (n = 5). (F) Double
735 immunofluorescence staining of microglia (Iba1, green) with M1 marker (CD68, red) in the
736 hippocampus. Nuclei were stained with Dapi. Scale bar: 50 μm. (G) Double immunofluorescence
737 staining of microglia (Iba1, green) with M2 marker (Arg-1, red) in the hippocampus. Nuclei were
738 stained with Dapi. Scale bar: 50 μm. (H) Quantification of the percentage of CD68 and Iba1
739 double-positive cells in the hippocampus (n = 4). (I) Quantification of the percentage of Arg-1 and
740 Iba1 double-positive cells in the hippocampus (n = 4). (J) Representative western blot images and
741 quantification of synaptic proteins including PSD95, SYN1, and BDNF in the hippocampus after
742 using T0901317 (n = 5). All data are presented as mean ± SEM. Two-way ANOVA, followed by
743 Turkey *post-hoc* test. *$P < 0.05$, **$P < 0.01$,***$P < 0.001$, ****$P < 0.0001$, ##$P < 0.01$, ###$P <$
744 0.001, ####$P < 0.0001$, n = 3-5 per group.
745

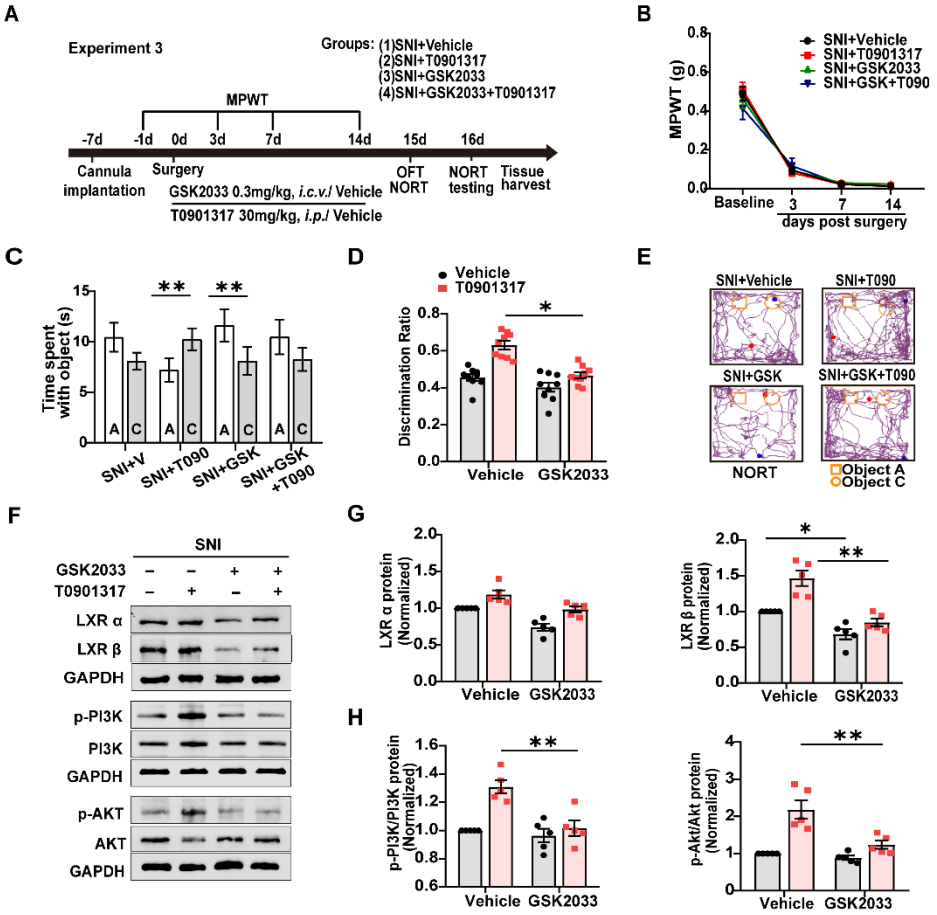

746

747 **Fig. 7 LXRs antagonist GSK2033 reversed the memory improvement induced by T0901317**

748 **in SNI mice** (A) Experimental designs and animal groups in administration of LXR antagonist

749 GSK2033 (0.3 mg/kg, *i.c.v.*) and agonist T0901317 (30 mg/kg, *i.p.*). (B) Mechanical allodynia

750 was evaluated by MPWT (n = 9). (C) Time spent with familiar object A and novel object C in the

751 NORT testing phase (n = 9). (D) Discrimination ratio in the NORT testing phase (n =9). (E)

752 Representative exploration traces in the NORT. (F-H) Representative western blot images and

753 quantification of LXRs and PI3K/AKT pathway-related proteins in the hippocampus of the SNI

754 group after using GSK2033 and T0901317 (n = 5). All data are presented as mean ± SEM. Two-

755 way ANOVA, followed by Turkey *post-hoc* test. *$P < 0.05$, **$P < 0.01$, n = 5-9 per group. GSK:

756 GSK2033.

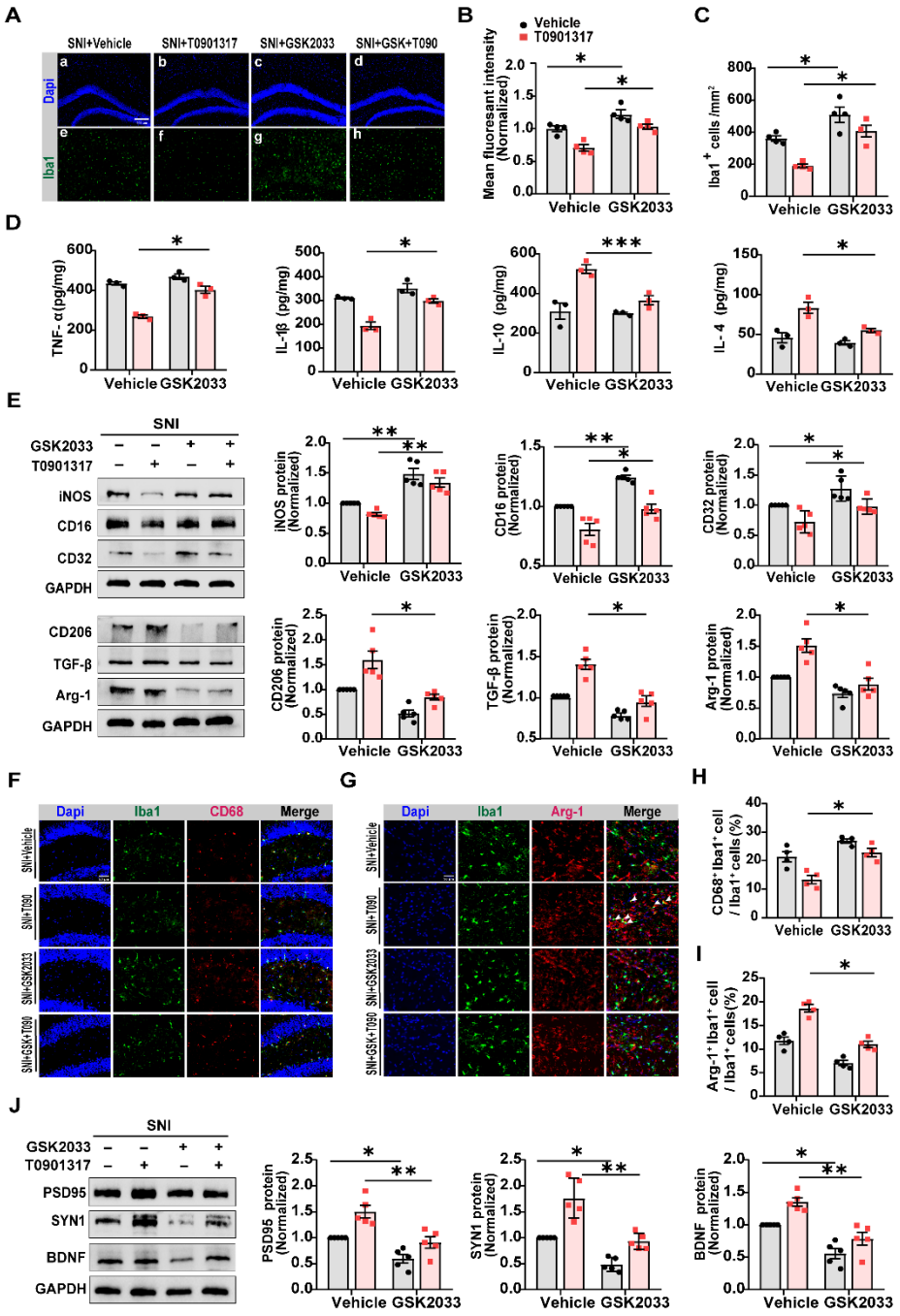

Fig. 8 Effects of LXRs antagonist GSK2033 on neuroinflammation, microglia polarization, and synaptic plasticity following T0901317 administration

(A) Representative images of immunofluorescence staining with Iba1 in the hippocampus sections after using GSK2033 and T0901317. Scale bar: 200 μm. (B) Quantification of the mean fluorescent intensity of Iba1-positive cells in the hippocampus (n = 4). (C) Quantification of the

763 number of Iba1-positive cells per square millimeter in the hippocampus (n = 4). (D) Measurement
764 of the levels of pro-inflammatory cytokines TNF-α, IL-1β, and anti-inflammatory cytokines IL-10,
765 IL-4 in the hippocampus after using GSK2033 and T0901317 (n = 3). (E) Representative western
766 blot images and quantification of expressions of M1 microglia markers iNOS, CD16, CD32, and
767 M2 markers CD206, TGF-β, and Arg-1 in the hippocampus (n = 5). (F) Double
768 immunofluorescence staining of microglia (Iba1, green) with M1 marker (CD68, red) in the
769 hippocampus. Nuclei were stained with Dapi. Scale bar: 50 μm. (G) Double immunofluorescence
770 staining of microglia (Iba1, green) with M2 marker (Arg-1, red) in the hippocampus. Nuclei were
771 stained with Dapi. Scale bar: 50 μm. (H) Quantification of the percentage of CD68 and Iba1
772 double-positive cells in the hippocampus (n = 4). (I) Quantification of the percentage of Arg-1 and
773 Iba1 double-positive cells in the hippocampus (n = 4). Nuclei were stained with Dapi. Scale bar:
774 50 μm. (J) Representative western blot images and quantification of synaptic proteins including
775 PSD95, SYN1, and BDNF in the hippocampus of SNI mice after using GSK2033 and T0901317
776 (n = 5). All data are presented as mean ± SEM. Two-way ANOVA, followed by Turkey *post-hoc*
777 test. *$P < 0.05$, **$P < 0.01$, ***$P < 0.001$, n = 3-5 per group.
778

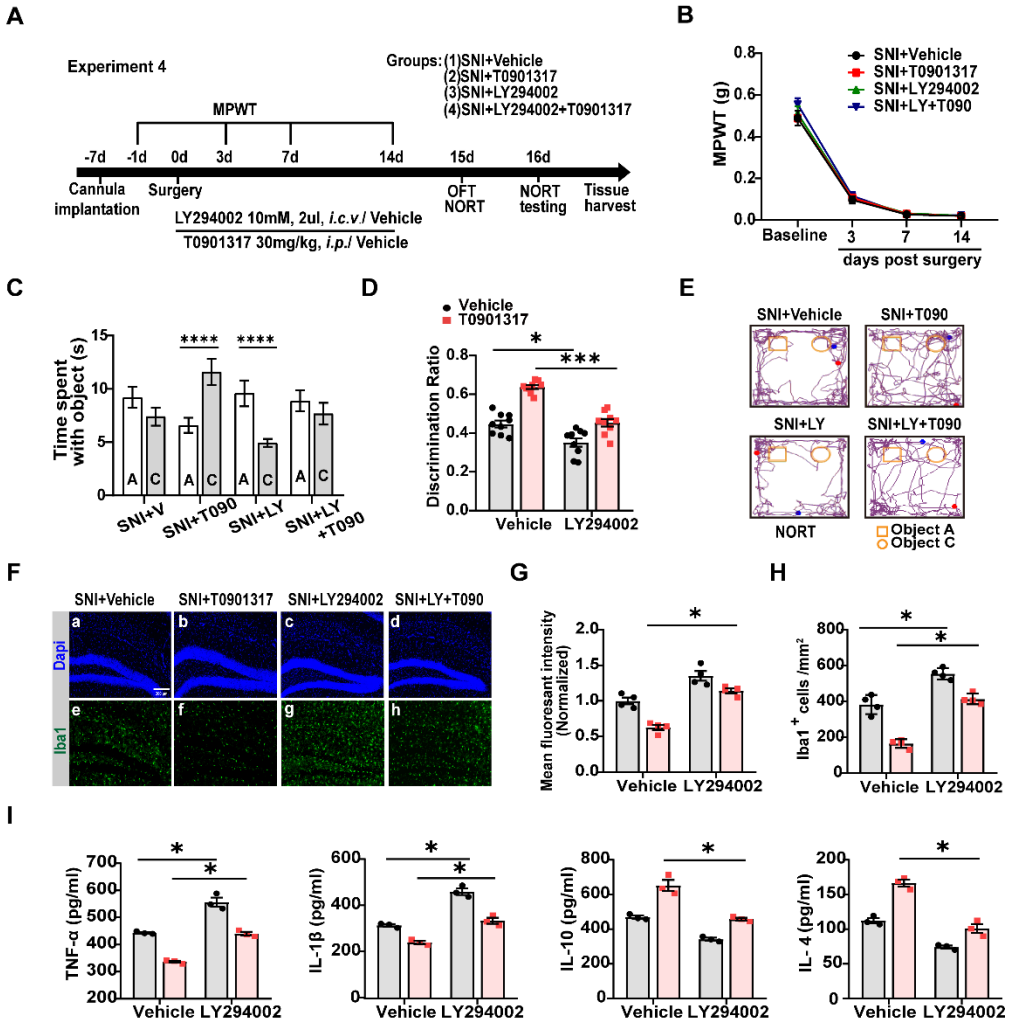

Fig. 9 PI3K inhibitor LY294002 blocked the cognitive improvement induced by T0901317 in SNI mice and exacerbated hippocampal neuroinflammation

(A) Experimental designs and animal groups after administration of PI3K inhibitor LY294002 (10mM, *i.c.v.*) and agonist T0901317 (30 mg/kg, *i.p.*). (B) Mechanical allodynia was evaluated by MPWT after using LY294002 and T0901317 (n = 9). (C) Time spent with familiar object A and novel object C in the NORT testing phase (n = 9). (D) Discrimination ratio in the NORT testing phase (n =9). (E) Representative exploration traces in the NORT. (F) Representative images of immunofluorescence staining with Iba1 in the hippocampus sections of SNI mice after using

LY294002 and T0901317. Scale bar: 200 μm. (G) Quantification of the mean fluorescent intensity of Iba1-positive cells in the hippocampus (n = 4). (H) Quantification of the number of Iba1-positive cells per square millimeter in the hippocampus (n = 4). (I) Measurement of the levels of pro-inflammatory cytokines TNF-α, IL-1β, and anti-inflammatory cytokines IL-10, IL-4 in the hippocampus after using LY294002 and T0901317 (n = 3). All data are presented as mean ± SEM. Two-way ANOVA, followed by Turkey *post-hoc* test. **P* < 0.05, ***P* < 0.01, ***P < 0.001, ****P < 0.0001. n = 3-9 per group. LY: LY294002.

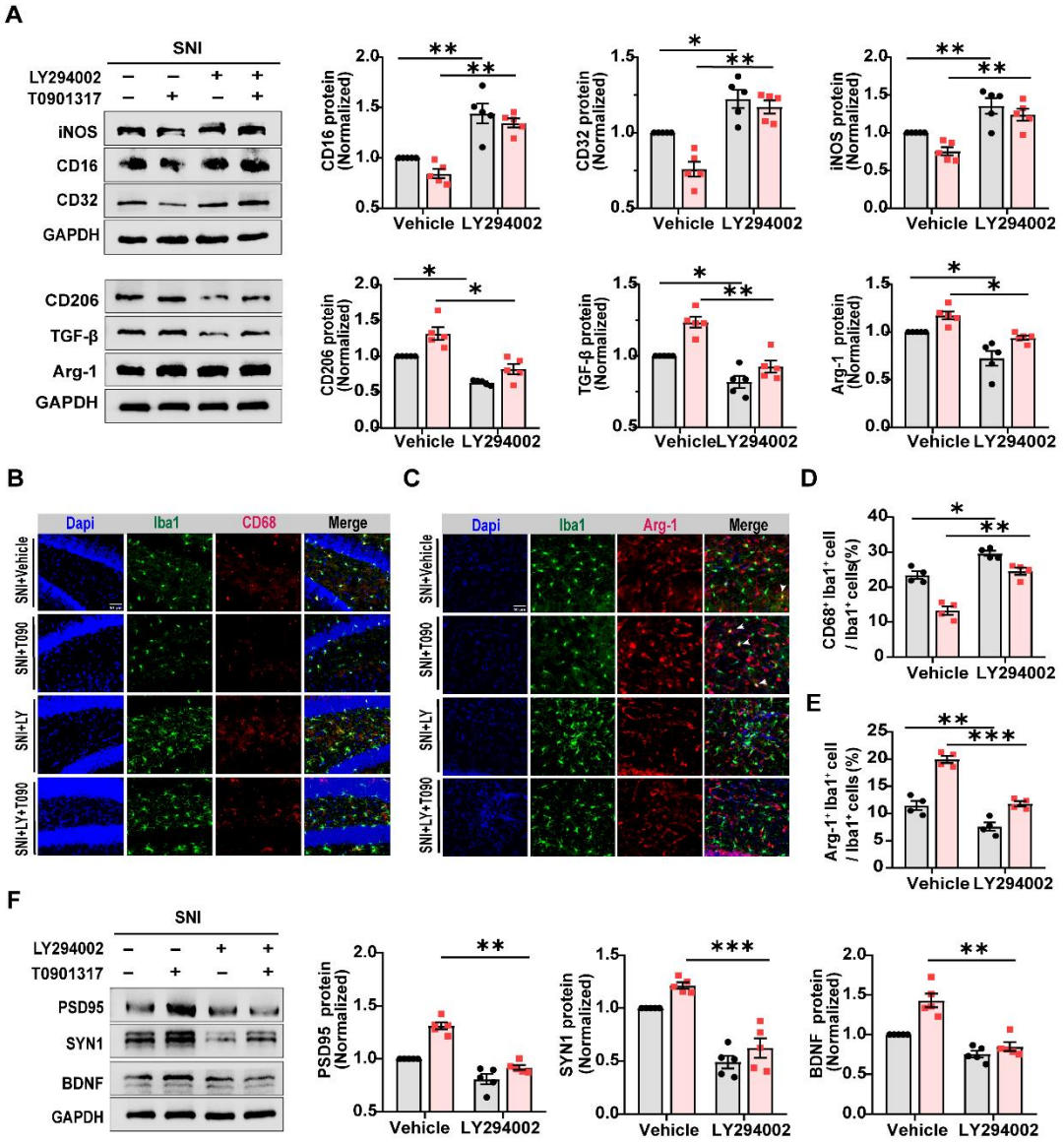

Fig. 10 Effects of PI3K inhibitor LY294002 on microglia polarization and synaptic plasticity following T0901317 administration in SNI mice

(A) Representative western blot images and quantification of expressions of M1 microglia markers iNOS, CD16, CD32, and M2 markers CD206, TGF-β, and Arg-1in the hippocampus of the SNI group after using LY294002 and T0901317 (n = 5). (B) Double immunofluorescence staining of microglia (Iba1, green) with M1 marker (CD68, red) in the hippocampus. Nuclei were stained with Dapi. Scale bar: 50 μm. (C) Double immunofluorescence staining of microglia (Iba1,

804 green) with M2 marker (Arg-1, red) in the hippocampus. Nuclei were stained with Dapi. Scale bar:
805 50 μm. (D) Quantification of the percentage of CD68 and Iba1 double-positive cells in the
806 hippocampus (n = 4). (E) Quantification of the percentage of Arg-1 and Iba1 double-positive cells
807 in the hippocampus (n = 4). (F) Representative western blot images and quantification of synaptic
808 proteins including PSD95, SYN1, and BDNF in the hippocampus after using LY294002 and
809 T0901317 (n = 5). All data are presented as mean ± SEM. Two-way ANOVA, followed by Turkey
810 *post-hoc* test. **P* < 0.05, ***P* < 0.01, ***P < 0.001. n = 4-5 per group.
811

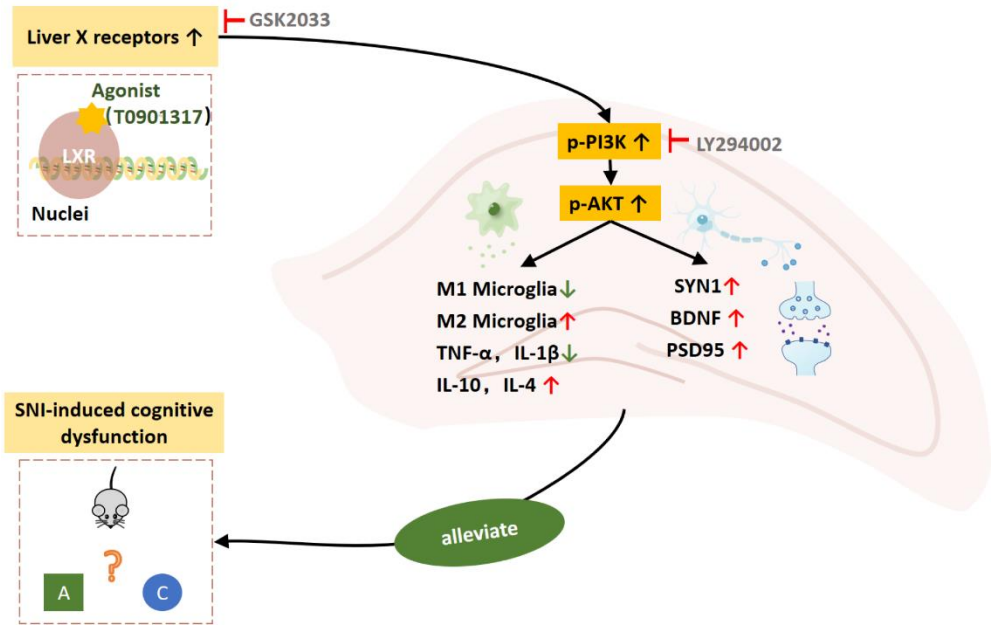

Fig.11 A schematic illustration of the proposed mechanism for activation of LXRs to alleviate neuropathic pain-induced cognitive dysfunction

Activation of LXRs by agonist T0901317 promoted microglia polarization from M1 to the M2 phenotype, attenuated inflammatory response, and increased synaptic proteins in the hippocampus via the PI3K/AKT signaling pathway, which eventually improved the neuropathic pain-induced cognitive dysfunction. The neuroprotective effects of T0901317 can be reversed by LXR antagonist GSK2033 and PI3K inhibitor LY294002.